| ISSN: 0001-5113<br>AADRAY | ACTA ADRIAT.,<br>54(1): 13 - 26, 2013 | |
|---|---|---|

# TerraSAR-X observations of the northeastern Adriatic bora: Early results

Milivoj KUZMIĆ[1*], Xiao-Ming LI[2], Branko GRISOGONO[3], Igor TOMAŽIĆ[1], and Susanne LEHNER[2]

*[1]Ruđer Bošković Institute, Division of Marine and Environmental Research, Satellite Oceanography Laboratory, Bijenička cesta 54, 10002 Zagreb, Croatia*

*[2]German Aerospace Center (DLR), Earth Observation Center (EOC), Remote Sensing Technology Institute (IMF), Oberpfaffenhofen D-82234 Wessling Germany*

*[3]University of Zagreb, Faculty of Science, Andrija Mohorovičić Geophysical Institute, Horvatovac bb, 10000 Zagreb, Croatia*

*[*]Corresponding author, e-mail: kuzmic@rudjer.irb.hr*

*Some early results of the TerraSAR-X observations of the northeastern Adriatic bora wind are presented in this paper. TerraSAR-X is a German X-band radar satellite launched in 2007 that carries phased array X-band synthetic aperture radar (SAR) operating in different polarizations and providing multiple imaging modes. SAR backscatter can be used to derive wind fields at spatial resolution that no other instrument can provide. Terrain-induced jet and wake patterns are particularly conductive to the SAR-instrument examination. Bora, a cold and dry downslope wind blowing from north-easterly directions on the eastern side of the Adriatic Sea, exhibits such a response. Since bora is primarily winter wind and the town of Senj is known for frequent and severe bora episodes we focus on TerraSAR-X scenes collected in the winters of 2011 and 2012 over an area with Senj roughly in its center. Recently developed XMOD2 geophysical model function is used for wind magnitude derivation, whereas the WRF model was employed to estimate the wind direction. The selected TerraSAR-X scenes have captured representative bora events exhibiting rich details in bora-induced jet and wake patterns on the lee of the Dinaric Alps. The details registered in the normalized radar cross section response strongly suggest the need for still higher resolution numerical simulations in order to properly model the orographic impact on and the fine details in the surface wind field. Comparisons with both research and operational modeling results indicate that the currently used geophysical model function may benefit from enlarging the matchup data base with samples of severe winds.*

**Key words:** TerraSAR-X, Adriatic, bora wind

## INTRODUCTION

TerraSAR-X is a German X-band radar satellite launched in 2007 in continuation of successful Space Shuttle missions, SIR-C/X and Shuttle Radar Topographic Mission. It carries an operational SAR system providing very high spatial resolution (down to 1 m). The instrument is a phased array X-band SAR, operating in different polarizations with beam steering capabilities, and providing multiple imaging modes like StripMap, Spotlight and ScanSAR (PITZ & MILLER, 2010; WERNINGHAUS & BUCKREUSS, 2010). The Spotlight mode provides 10 km x 10 km scene at spatial resolution of 1-2 m, the StripMap mode generates 30 km wide strips with resolution between 3 and 6 m, whereas the ScanSAR mode delivers 100 km wide strips with resolution of 17 m. Basic sensor information is summarized in Fig. 1. More information about the sensor can be found in BREIT *et al.* (2007). Those capabilities make the sensor a very interesting tool for oceanography as well as meteorology, with high-resolution near-surface wind field being of interest for both.

There are several approaches to estimating the wind parameters from SAR images of the sea surface (LIN *et al.*, 2008). SAR-wind derivation is essentially empirical, relaying on the concept of geophysical model function (GMF), originally developed for the ocean wind scatterometry. The GMFs, relating the measured normalized radar cross section ($\sigma^o$) to the wind speed and direction and the SAR-scene geometry, are commonly used to retrieve the sea surface wind field (e.g. LEHNER *et al.*, 1998; MONALDO, 2000; LI *et al.*, 2007). Early SAR instruments (e.g. on ERS-1/2, RADARSAT-1/2, or ENVISAT) have employed the C band, so several GMFs were developed and validated for the C-band instruments, e.g. CMOD-4 (STOFFELEN & ANDERSON, 1997), CMOD_IFR2 (QUILFEN *et al.*, 1998), or CMOD5 (HERSBACH *et al.*, 2007). Inversion of the GMF does not uniquely relate the $\sigma^o$ to SAR-derived wind magnitude; the missing directional information is commonly estimated internally, from orientation of low frequency coherent structures in the SAR image, or externally, from scatterometer measurements or atmospheric model output (MONALDO *et al.,* 2003). HORSTMANN & KOCH (2005), for example, developed a methodology for high resolution ocean surface wind retrieval from C band SAR data employing several GMF models. To derive wind from the X-band Ter-

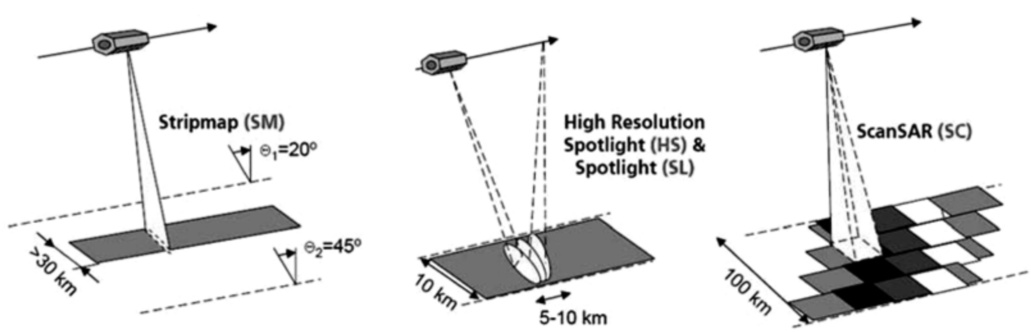


| | Stripmap | Spotlight (HS & SL) | ScanSAR |
|---|---|---|---|
| *swath width* | 30 km (single & twin pol.)<br>15 km (dual & quad pol.) | 10 km @ *150 MHz chirp BW*<br>azimuth: 5 / 10 km (HS / SL) | 100 km |
| *full performance incidence angle range* | 20° - 45° | 20° - 55° | 20° - 45° |
| *azimuth resolution* | 3 m (single pol.)<br>6 m (**dual pol.**) | 1 m / 2 m (HS , single / **dual pol.**)<br>2 m / 4 m (SL , single / **dual pol.**) | 17 m<br>(1 look, 4 beams) |
| *ground range resolution @ 150 MHz chirp BW* | 1.7 m - 3.5 m (@ 45°.. 20°) | 1.5 m - 3.5 m (@ 55°..20°) | 1.7 m - 3.5 m (@ 45°.. 20°) |

*Fig. 1. The TerraSAR-X operating modes. Adopted from LEHNER et al., (2008), Copyright DLR*

raSAR data a new GMF, named XMOD1, was developed (REN *et al.*, 2012). Applications of the XMOD1 to obtain high resolution sea surface wind field from the TerraSAR-X data, particularly in coastal areas, have been reported in REN *et al.* (2012) and LEHNER *et al.* (2012).

The SAR backscatter, strongly related to the sea surface roughness, can be used to derive wind fields at spatial resolution that no other instrument can provide, thereby potentially revealing horizontal wind variability unavailable by other means. Terrain-induced low-level jet and wake patterns are particularly conductive to the SAR-instrument examination. A case in point is bora, a cold and dry downslope wind blowing from north-easterly directions on the eastern side of the Adriatic Sea. Bora subtleties, like its varying strength or interactions of different mechanisms, are not fully understood yet, but solid understanding of its basic nature for the strong to severe cases does exist. A recent review of advances in the understandings of severe bora flows is found in GRISOGONO & BELUŠIĆ (2009). Bora onset and development relate to orographic wave steepening, overturning and eventual breaking, often yielding hydraulic jump-like flow structure in the lee of a mountain (SMITH, 1987; KLEMP & DURRAN, 1987; ENGER & GRISOGONO, 1998; GRISOGONO & BELUŠIĆ, 2009). There is a multitude of (sub)mesoscale processes and phenomena that pertain to bora flows that have been studied in details recently: vigorous gustiness, boundary-layer variations, jets and wakes, rotors, pulsations, etc. (BELUŠIĆ & KLAIĆ, 2004, 2006; GRISOGONO & ENGER, 2004; GRUBIŠIĆ, 2004; BELUŠIĆ *et al,*. 2007; GOHM *et al.,* 2008). HORVATH *et al.*(2011) indicate that bora airflows are often different at the central and southern Adriatic, compared to those over the north-eastern Adriatic, mostly because of the more complex southern terrain. Furthermore, fine-scale bora processes and ultimately bora turbulence characteristics are addressed nowadays as well (VEČENAJ *et al.,* 2010, 2012). It is the fine-scale where high-resolution sensors like TerraSAR-X can prove particularly useful. Furthermore, fine-scale resolving atmospheric forcing is essential for the Adriatic Sea due to laterally highly variable fluxes at the air-sea interface (KUZMIĆ & ORLIĆ, 1987; ORLIĆ *et al.,* 1994; PULLEN *et al.*, 2003).

The goal of the paper is two-fold. We aim to explore the utility of high-resolution X-band SAR data in mapping the bora wind, the TerraSAR-X in particular, and to use a high-resolution atmospheric model derived wind direction in order to avoid problems with internal wind direction derivation in low backscatter areas. The paper is organized as follows. After the introduction we briefly present the TerraSAR-X data processing, and the atmospheric model used to provide the wind direction. Four recent bora episodes acquired with the TerraSAR-X are presented and discussed in the third section. The work is summarized and the conclusions drawn in the final section.

## SATELLITE DATA AND NUMERICAL MODEL

In this work we focus on four TerraSAR-X scenes recently collected over the northeastern Adriatic Sea within the framework of the proposal OCE0478, "TerraSAR observations and mathe- matical modeling of the Adriatic bora wind and related wave field". The scenes principal parameters are summarized in Table 1; maps of the scenes geographic coverage are given in Fig. 2. The February 25, 2011 scene was acquired in StripMap mode (nominal resolution 3-6 m) whereas the other three were acquired in ScanSAR mode (nominal resolution 16 m). To derive wind from the X-band TerraSAR data the XMOD2 GMF was used (LI & LEHNER, 2013), which has the similar model functions to the CMOD5, i.e.

$$z(U_{10},\varphi,\theta)=B_0^p(U_{10},\theta)\left(1+\sum_{k=1}^{2}B_k(U_{10},\theta)\cos(k\varphi)\right) \quad (1)$$

where $z=(\sigma^0)^p$ , $p = 0.625$, $U_{10}$ is the wind speed at 10 m height above the sea surface given in $ms^{-1}$, $\theta$ is the incident angle given in degrees, and $\varphi$ is the angle of wind direction relative to the radar azimuth; Both $B_1$ and $B_2$ are functions of the wind speed and incidence angle. The equation (1) is cast in a transformed, $z$ space, whereas the original XMOD1 equation is tuned in the *dB* space:

$$\sigma^0(U_{10},\theta,\varphi)=x_0+x_1\,U_{10}+x_2\sin(\theta)+x_3\cos(2\varphi)+x_4\,U_{10}\cos(2\varphi)\quad(2)$$

with $dB \equiv 10\log(\sigma_0) \equiv 16\log(z)$

The symbols $U_{10}$, $\theta$ and $\varphi$ have the same meaning as those in the equation (1); the $x_i$ are the coefficients determined using the tuning dataset.

As pointed out in the introduction, commonly employed GMFs require wind direction to facilitate inversion to derive the wind speed. Features in an image, aligned with the wind, can

*Table 1. Technical characteristics of the analyzed TerraSAR-X scenes*

| Date | Start Time | Stop Time | Mode | Polarization | Direction | Orbit No |
|---|---|---|---|---|---|---|
| 25.02.2011 | 16:41:54.98 | 16:42:02.98 | StripMap | VV | Ascending | 3790 |
| 22.03.2011 | 05:10:05.22 | 05:10:27.22 | ScanSAR | VV | Descending | 20892 |
| 04.02.2012 | 05:10:08.30 | 05:10:30.30 | ScanSAR | VV | Descending | 25735 |
| 12.02.2012 | 16:41:53.31 | 16:42:15.31 | ScanSAR | VV | Ascending | 25864 |

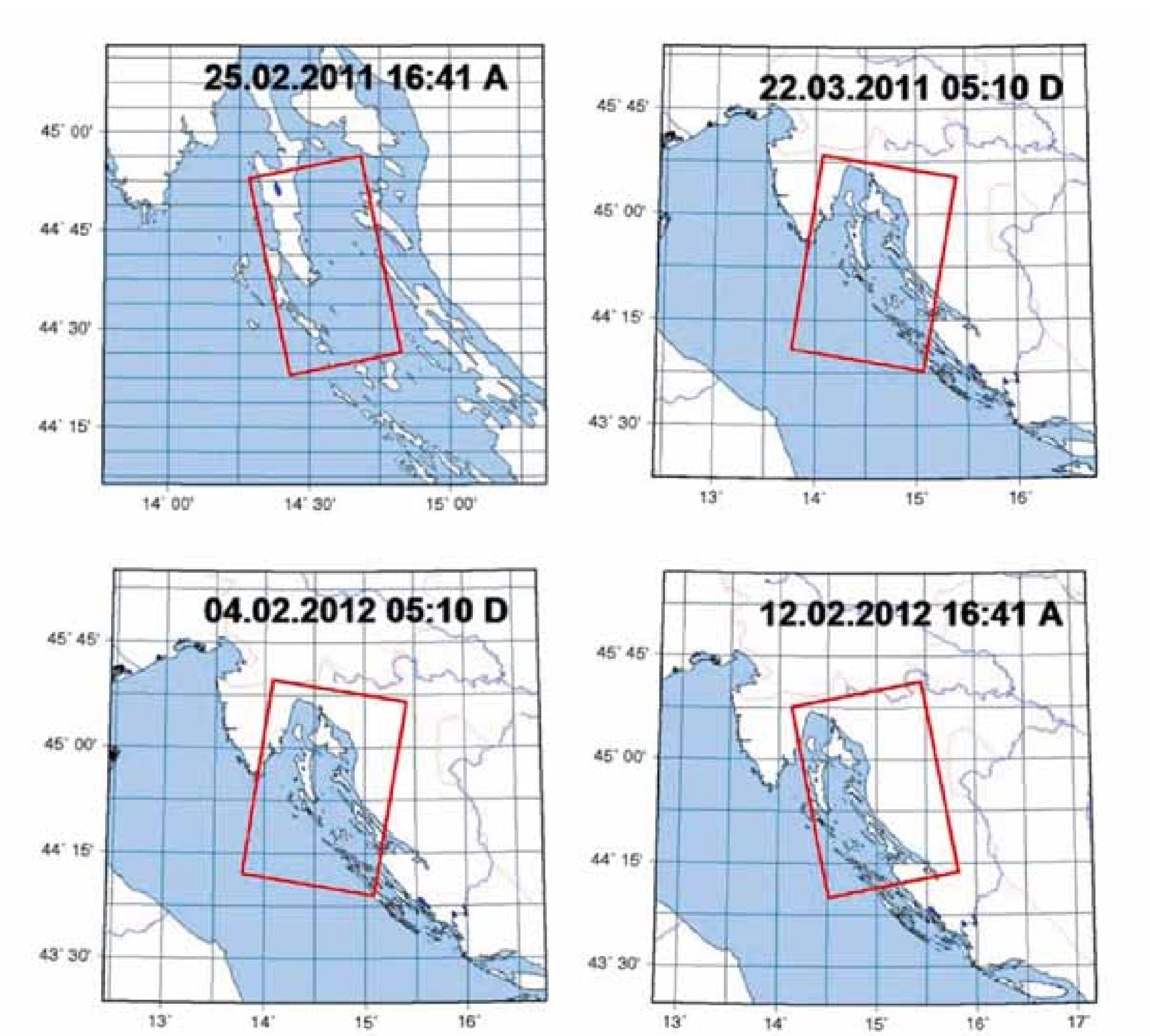


*Fig. 2. Geographic coverage of the selected TerraSAR-X images; red squares mark scene boundaries. Letter A stands for ascending, and letter D for descending orbit*

be used to extract wind direction from the image itself, via either spectral or spatial domain methods (e.g. LIN *et al.*, 2008). Ambiguities in isolated useful features or featureless regions can degrade or impair the quality of thus derived directional information. Alternatively, external source, like wind scatterometer or numerical model, can be used to provide the needed directional information. In the present study the TerraSAR-X wind fields were derived using the wind direction from an atmospheric model. The regional meteorological model used to obtain the 10 m wind direction is the Weather Research and Forecasting (WRF) model with the Advanced Research WRF dynamic core, version 3.2 (SKAMAROCK *et al.*, 2008). WRF is a next-generation, limited-area, non-hydrostatic, mesoscale modeling system with terrain following vertical eta-coordinate. Three one-way nested model domains are used with a horizontal mesh size of 16.0 km (78x72), 4.0 km (121x117), and 1330 m (118x133), respectively; the third domain was used in TerraSAR-X wind derivation. The area covered by the domains together with a close-up of the third domain is presented in Fig. 3. Also plotted in the figure is the orography. The outermost model domain (size of approximately 1250x 1150 km$^2$) is centered at 45.03°N and 14.65°E, with the third domain roughly centered on the town of Senj. Forty tangent-hyperbolic stretched terrain-following hydrostatic pressure levels were used in the vertical, with a constant pressure at the model top set to 50 hPa. Initial and boundary conditions were obtained from the European Centre for Medium-Range Weather Forecasts (ECMWF) analyses in the Meteorological Archive and Retrieval System (MARS). Horizontal resolution of the dataset is 0.141° (T1279). Ninety-one model level data were used to prepare the input. The model was initialized at 0000 UTC each day and run for 72 h, updating the boundary conditions every six hours and recording output data every hour in the domain used to derive wind direction. Grid

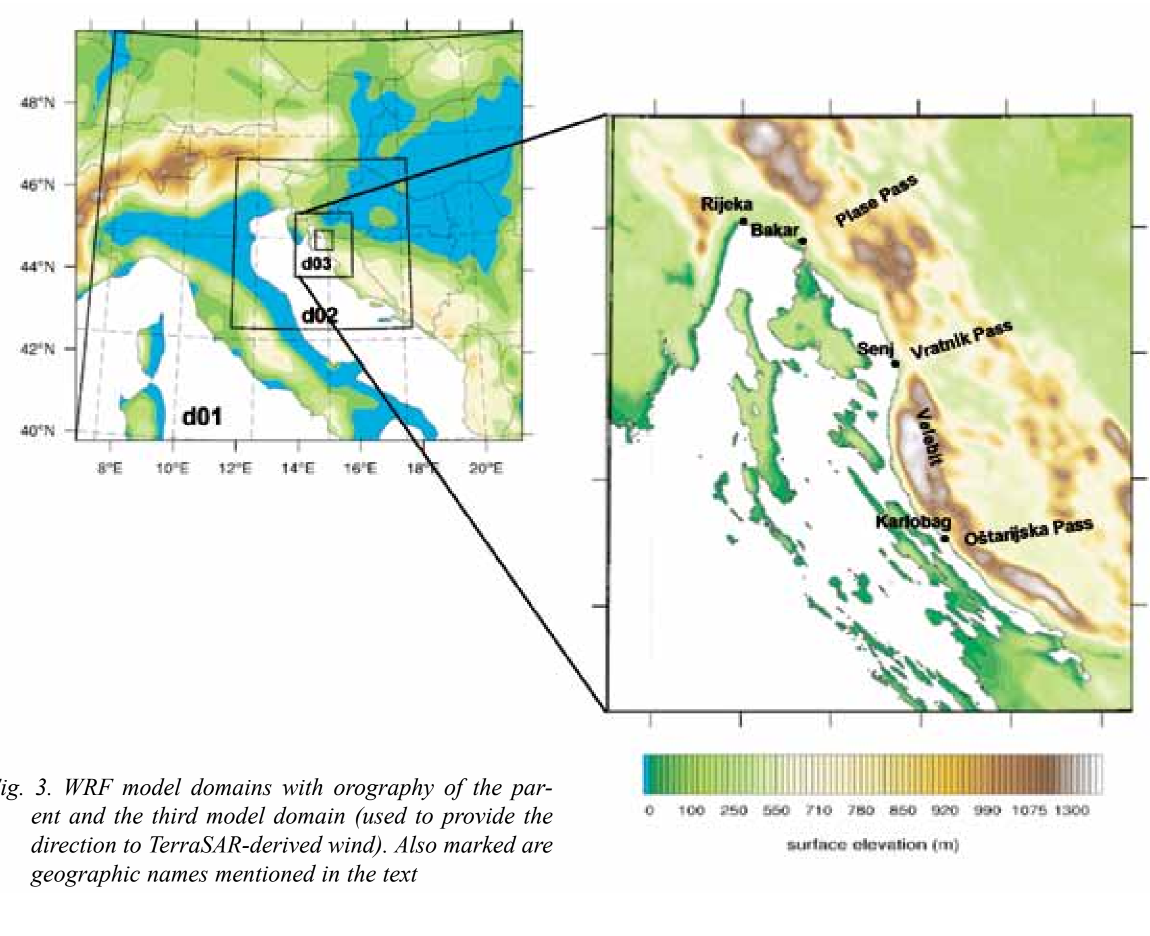


*Fig. 3. WRF model domains with orography of the parent and the third model domain (used to provide the direction to TerraSAR-derived wind). Also marked are geographic names mentioned in the text*

analysis nudging was applied in the outermost domain. The procedure was repeated for each TSX episode, to provide the 10 m wind field on the scene recording hour. In all domains the Thompson graupel scheme was adopted for microphysics. The longwave and shortwave radiation schemes are based on RRTM and Goddard short wave schemes, respectively. Unified Noah land-surface model (CHEN & DUDHIA, 2001) with 4 soil layers was the land-surface option. A modified version of the KAIN & FRITSCH (1993) scheme was employed for the cumulus parameterization in the outermost domain, and no cumulus option in the two innermost domains. The Mellor-Yamada-Janjic PBL parameterization was used in all domains. Described setup was deemed suitable for calculation of the wind direction needed to derive the SAR wind. To that end wind direction from the innermost, third domain (see Fig. 3), calculated at 1330 m resolution, was downscaled to the 500 m resolution of the spatially averaged normalized radar cross section (NRCS) grid and then used to retrieve the surface wind. For the sake of later comparison we provide in Fig. 4 the WRF hindcasts of both the wind magnitude and direction, for the TSX image dates and the hours closest to the scenes acquisition time.

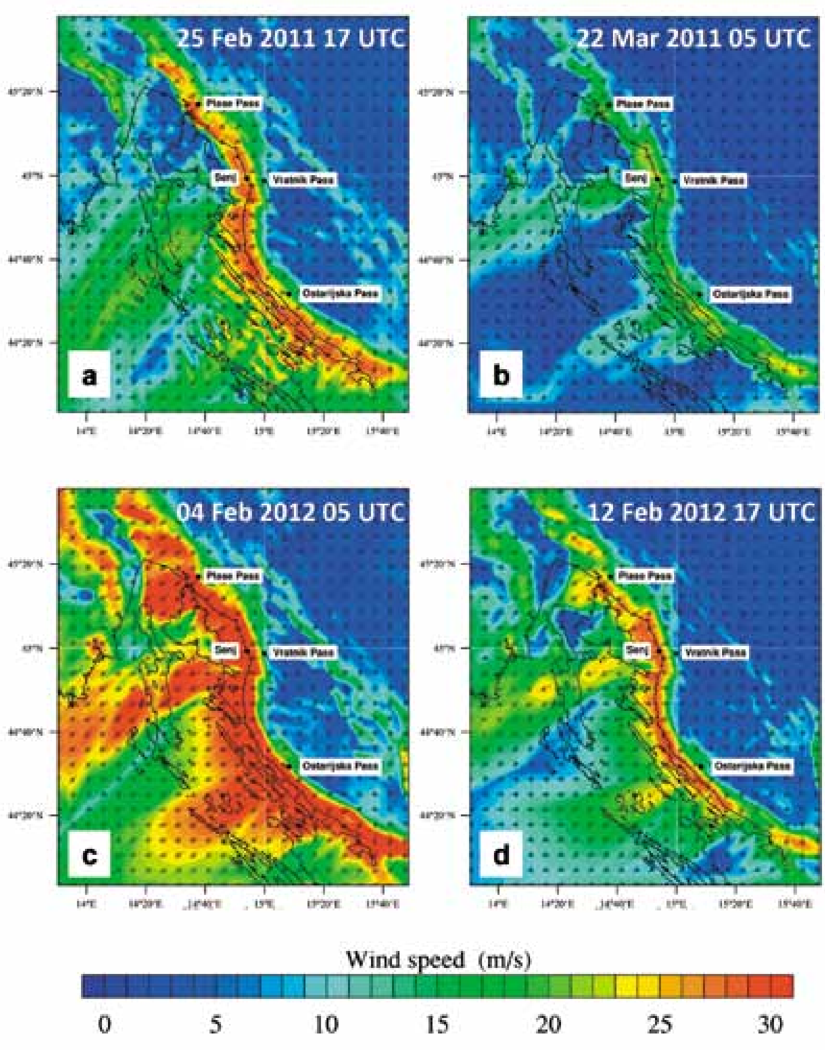


*Fig. 4 Third WRF model domain (see Fig. 3) hindcast of 10 m wind magnitude and direction for: (a) 25 February 2011, 17 UTC; (b) 22 March 2011, 05 UTC; (c) 4 February 2012, 05 UTC; (d) 12 February 2012, 17 UTC. The spatial resolution is 1330 m, but not every grid vector is plotted*

## RESULTS AND DISCUSSION

There are three elements important to Adriatic bora development. One is high-pressure center over the continental Europe, providing inflow of colder air masses. Such an anti-cyclone is often accompanied by the second element: a cyclone traveling over the Adriatic Sea. The third element is a mountain range between these centers: the Dinaric Alps. Depending on prevailing synoptic pattern bora is called cyclonic or anti-cyclonic. Yet another type, short lasting frontal bora, may be induced by a passage of a cold front (GRISOGONO & BELUŠIĆ, 2009). With either anti-cyclone push or cyclone pull of the air masses, the net result is a pressure gradient across the mountain barrier and strong downslope wind on its lee side. Gaps and peaks in the barrier act to develop bands of jets and wakes. Orographic wave breaking turns out to be the important mechanism in the jet and wakes development (JIANG & DOYLE, 2005): wave breaking in the lee of high terrain induces wakes; minimized breaking in the lee of the gaps produces fast-flow layers, extending further downstream. A SAR instrument with its high resolution imaging of wind-induced surface roughness is very useful tool in exploring the impact of bora on the Adriatic Sea. In what follows we will use four recent Adriatic bora events to demonstrate capabilities of the TerraSAR-X instrument in this context. In a previous paper (SIGNELL *et al.*, 2010) authors stress the capability of the SAR sensor to resolve sub-kilometer details of the Adriatic bora jets. Their conclusions were based on an analysis of ten spatially averaged RADARSAT-derived images. ALPERS *et al.* (2009) comparatively explored bora events over the Adriatic Sea and Black Sea using the SAR images acquired by the Advanced SAR (ASAR) instrument on-board the European ENVISAT. They also found the SAR instrument

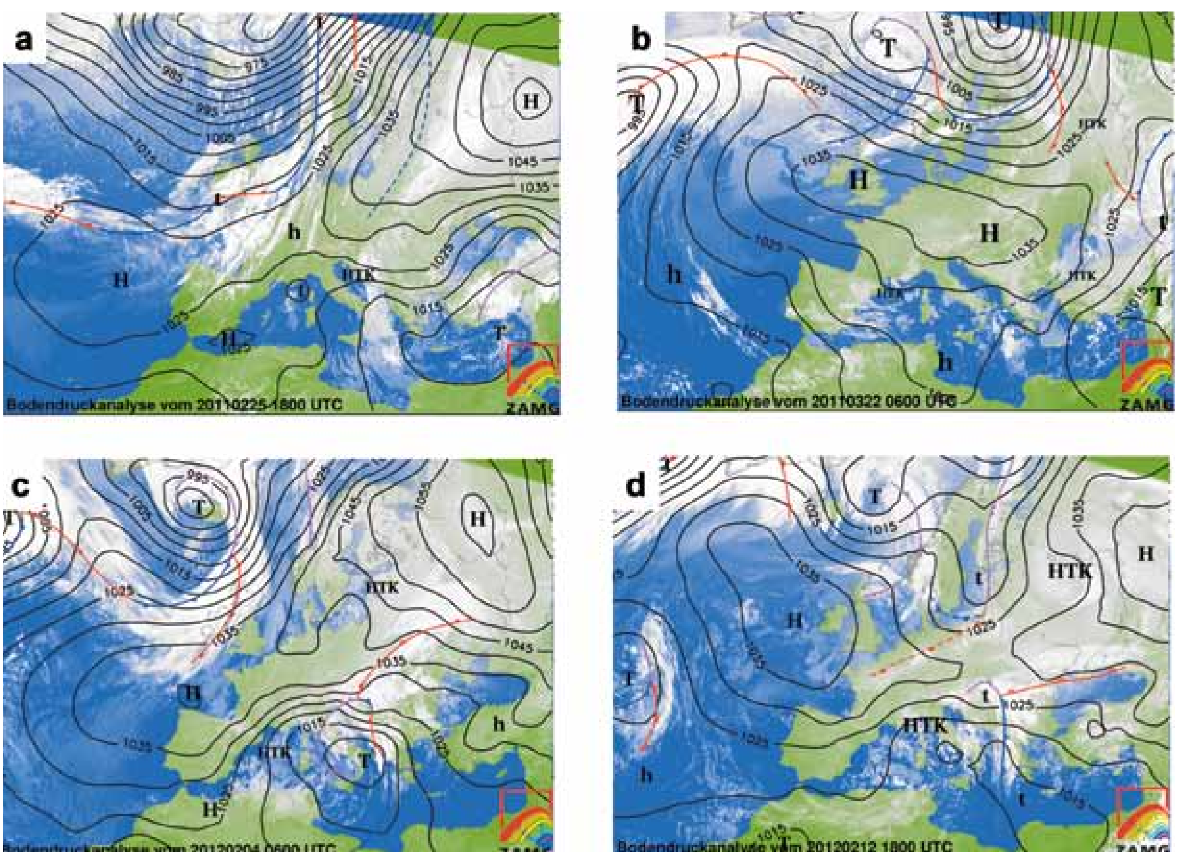


*Fig. 5. Charts of the sea-level pressure on the days on which selected TerraSAR-X scenes were registered. Copyright ZentralAnstaldt fur Meteorologie und Geodynamik*

capable of resolving bora-induced wind jets and wakes, and stressed in particular its potential usefulness in validation and improvement of mesoscale atmospheric models simulating bora events. The TerraSAR-X sensor has operating modes with high resolution offering possibility for observing and examination of the fine-scale structure of the bora jets and wakes. Bora is more frequent and energetic in winter, and the town of Senj (Fig. 3) is known for particularly severe and persistent bora events (e.g. SMITH, 1987). We therefore focus on four bora events that took place in the winters of 2011 and 2012 over the northeastern Adriatic, on the lee of the part of Dinaric Alps stretching from Rijeka to Karlobag, with Senj positioned half-way (Fig. 3).

### 25 February 2011, 1800 UTC

In this case an anti-cyclonic bora flow developed under influence of the high-pressure system centered west of the Ural area (Russia), connected with the high-pressure over the Western Europe and assisted by a cutoff low passing east of the Alps, over the Northern Adriatic toward Sicily (Fig. 5a). During this case a weak depression developed southwest of the Alps and got locked in phase with the cutoff low for the next two days, eventually dissipating. In response to this situation bora wind developed in the lee of the Dinaric Alps; a snapshot of the event was registered by the TerraSAR-X sensor on February 25 (Fig. 6). In Fig. 6a the NRCS is plotted, overlaid with the WRF-derived directional vectors, whereas in Fig. 6b SAR derived wind field is laid out. The normalized radar cross section response in the northern (brighter) part of the scene is stronger than in the southern (darker) which respectively translates into higher and lower wind velocities seen in the Fig. 6b. Relatively small extent of this scene (30 km x 55 km - the only one of the four scenes that was acquired in the StripMap mode) combined with its more offshore position prevented simultaneous registration of the situation near coast, but

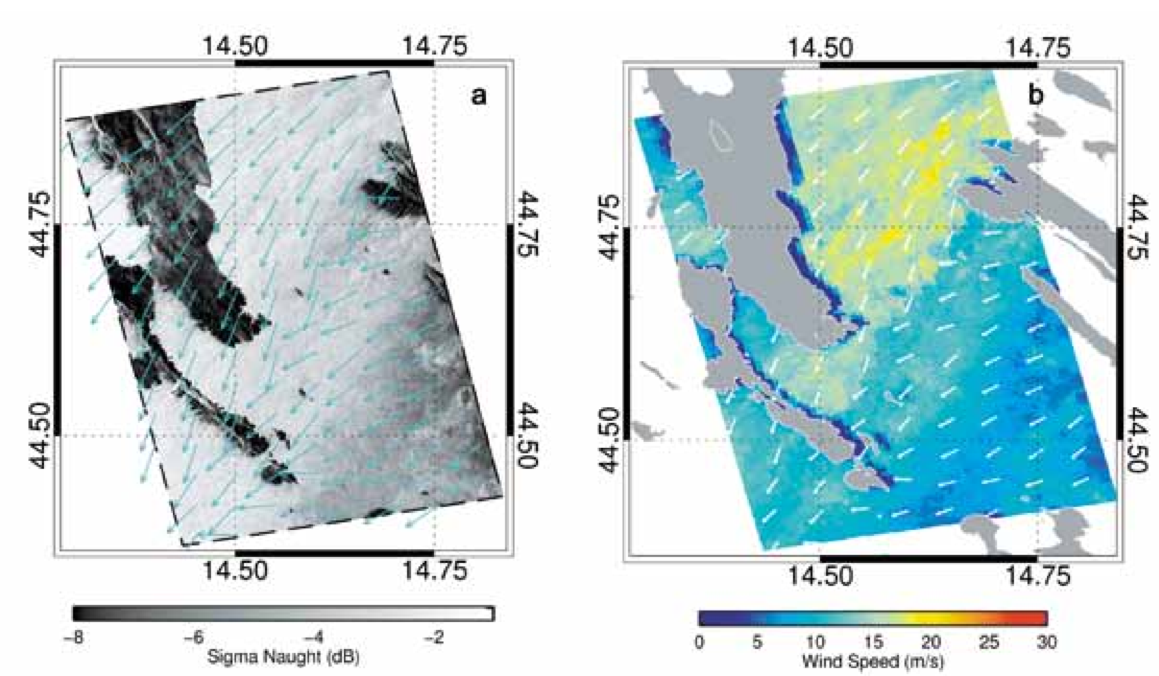


*Fig. 6. (a) Normalized radar cross-section and (b) TerraSAR-X derived 10 m wind field for 25 February 2011, 16:41 UTC. The color palette is used to represent the wind magnitude in (b). The same model directional information overlays both parts of the figure, although it is differently presented graphically in (a) and (b). The WRF model 3rd domain (horizontal resolution 1330 m) was interpolated on the 500 m NRCS grid to provide the wind direction. Direction-indication vectors are plotted on the native WRF model grid in (a), and on the NRCS grid in (b). The scene incidence angle range is 19.7 – 23.1 degrees*

the WRF model simulation (Fig. 4a) indicates that the brighter and darker parts of the scene can be related to the Senj jet and Velebit wake respectively (see Fig. 3). The relation of the jet-and-wake pattern to the pass-and-peak sequence is better seen in the other three ScanSAR scenes.

**22 March 2011, 0600 UTC**

The next case is characterized by high-pressure systems over Russia and central Western Europe (related again to the Siberian and Azorean anti-cyclone, respectively) (Fig. 5b). A deep elevated trough developed over the central Mediterranean and a cutoff low over the SE Scandinavia, promoting cold air advection from the Central Europe toward the northeastern Adriatic. Again, bora wind developed in the lee of the Croatian coastal ridge (Fig. 7). In the NRSC field (Fig. 7a) a string of jets and wakes is clearly observed. Jets develop downstream of the passes in the mountain ridge, whereas downstream of mountain peaks surface wakes are created (GRUBIŠIĆ, 2004). A prominent jet develops downstream of the Vratnik Pass, in the Senj hinterland (Fig. 3), but weaker jet is observed north of it, emanating from the Plase Pass (Fig. 3) while two more jets are visible south of the Senj jet. The dominant wake area is the one downstream of the Velebit mountain while smaller wakes are noted, separating the mentioned jets. A previous study (JIANG & DOYLE, 2005) connected surface jet and wake formation with the mountain wave breaking aloft. It is worth noting that the WRF model predicts rather well position and extent of the jets and wakes (Fig. 4b), as well as the wind magnitude of somewhat lower intensity compared to the three other analyzed cases).

**04 February 2012, 0600 UTC**

This case is a predominantly cyclonic-bora event (with some frontal and anti-cyclonic elements) associated with a persistent, higher-level trough stretching from the southeast Scandinavia to the Western Mediterranean area. In addition to this synoptic setup, the Azorean high-pressure ridge extended out over the Western Europe, including some of its central parts, connecting to the exceptionally strong Siberian anti-cyclone (Fig. 5c). As the sub-synoptic cyclonic

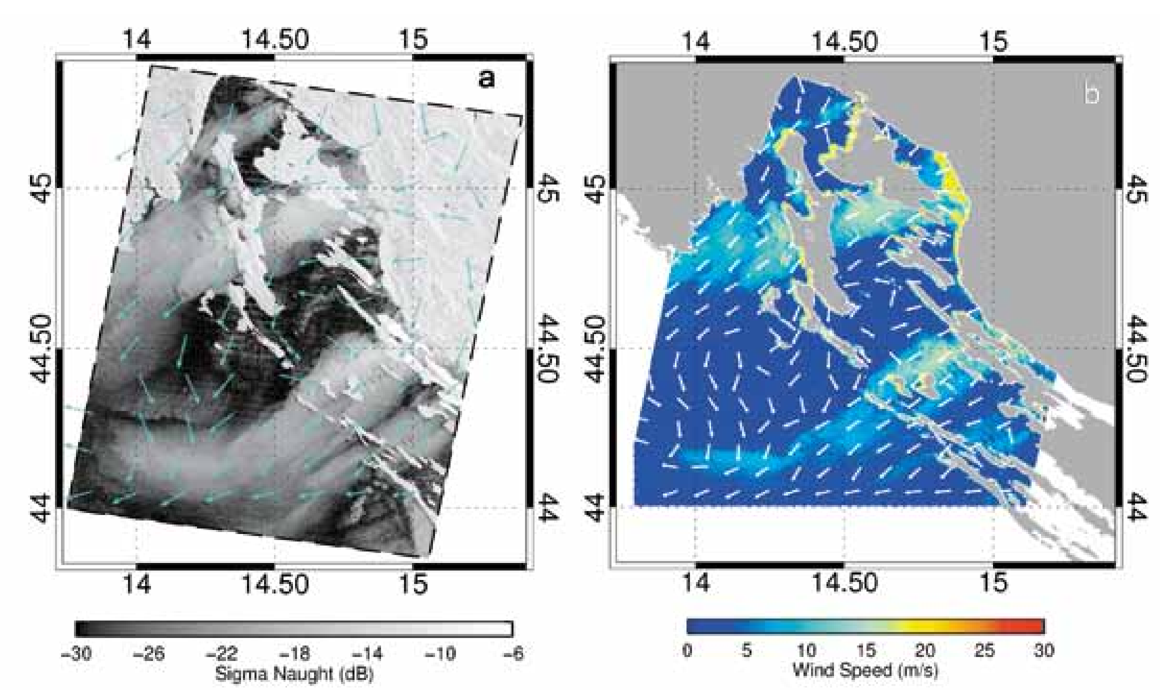


*Fig. 7. As in Fig. 6, but for 22 March 2011, 05:10 UTC. The scene incidence angle range is 37.9 – 45.6 degrees*

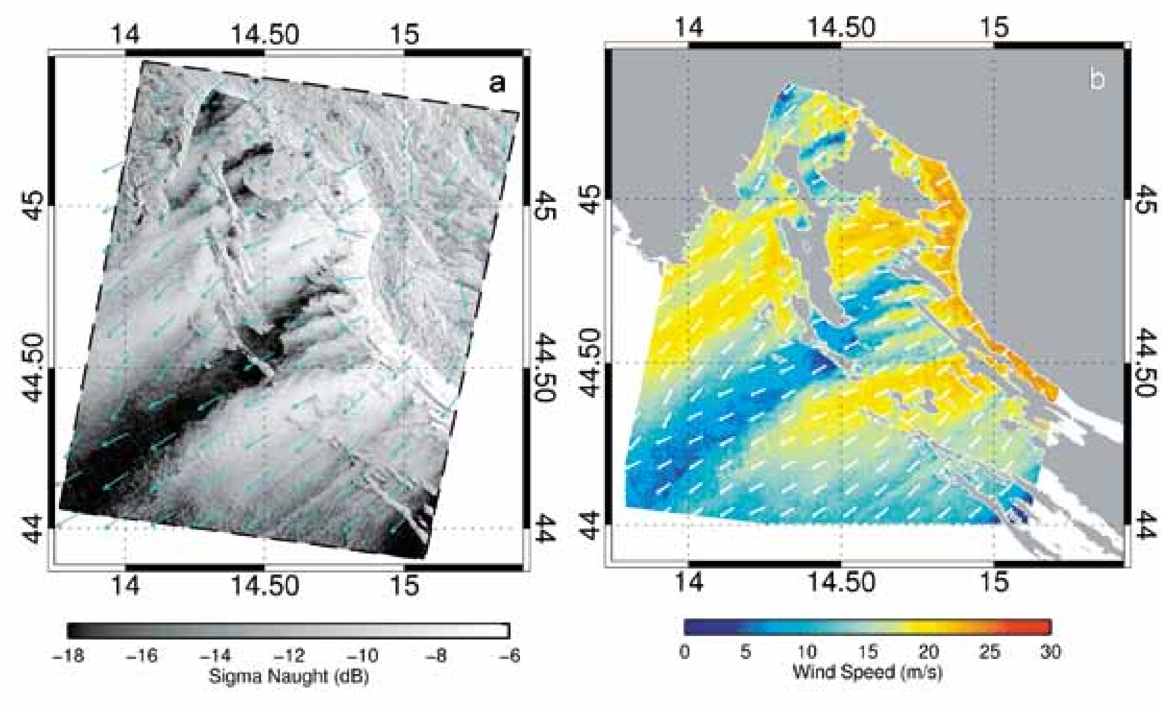


*Fig. 8. As in Fig. 6, but for 4 February 2012, 05:10 UTC. The scene incidence angle range is 37.9 – 45.6 degrees*

activity moved from Italy eastward over the Adriatic Sea, under gradual filling, its frontal system developed with an occluded front east of the Adriatic. The cyclone persisted over the area associated with the higher-level trough; later on, it expanded and reactivated toward the Northern Africa while mingling in the central Mediterranean. Meanwhile, the near-surface high-pressure linkage between the Western Europe and Siberian anti-cyclone persisted throughout the period (with a brief weakening interval). This case is particularly interesting as the long-lasting overall situation brought for the broader Adriatic region the coldest part of the whole winter. The described characteristics are reflected in the registered TerraSAR-X scene (Fig. 8). The increased brightness of the Senj and Karlobag jets (Fig. 8a) suggests much higher velocities, with the Bakar jet also exhibiting higher intensity. Noteworthy are the three smaller jets between the Senj and Karlobag ones, in an area usually occupied by the Velebit wake. Their appearance suggests unusual intensity of the air flow over the Velebit Mountain, as much as it testifies to the ability of the TerraSAR-X sensor to detect such details. The derived wind is strong, but both the WRF (Fig. 4c) and the Croatian operational model (not shown) predictions suggest that the wind was even stronger. It is worth noting here that the XMOD2 GMF coefficients were derived from a matchup base with wind data samples not including severe winds, therefore exhibiting possible bias towards weaker winds, so the actual wind in this case indeed may have been stronger. Comparing this case to that of the March 22$^{nd}$ 2011 one notes strong intensification of the major jets and development of a string of smaller and shorter ones near the coast. It appears almost as if the Dinaric Alps were not high enough barrier in this case.

**12 February 2012, 1800 UTC**

In our final case an anti-cyclonic bora type dominates over the Northern Adriatic while the central eastern Adriatic coast experiences cyclonic and (occluded) frontal bora-type flow. The long-lasting elevated depression split into two more remote cutoff-lows further apart (the remnants of the previous February 4 case) allowing for a persistent high-pressure system over the central Europe (Fig. 5d). Meanwhile, the

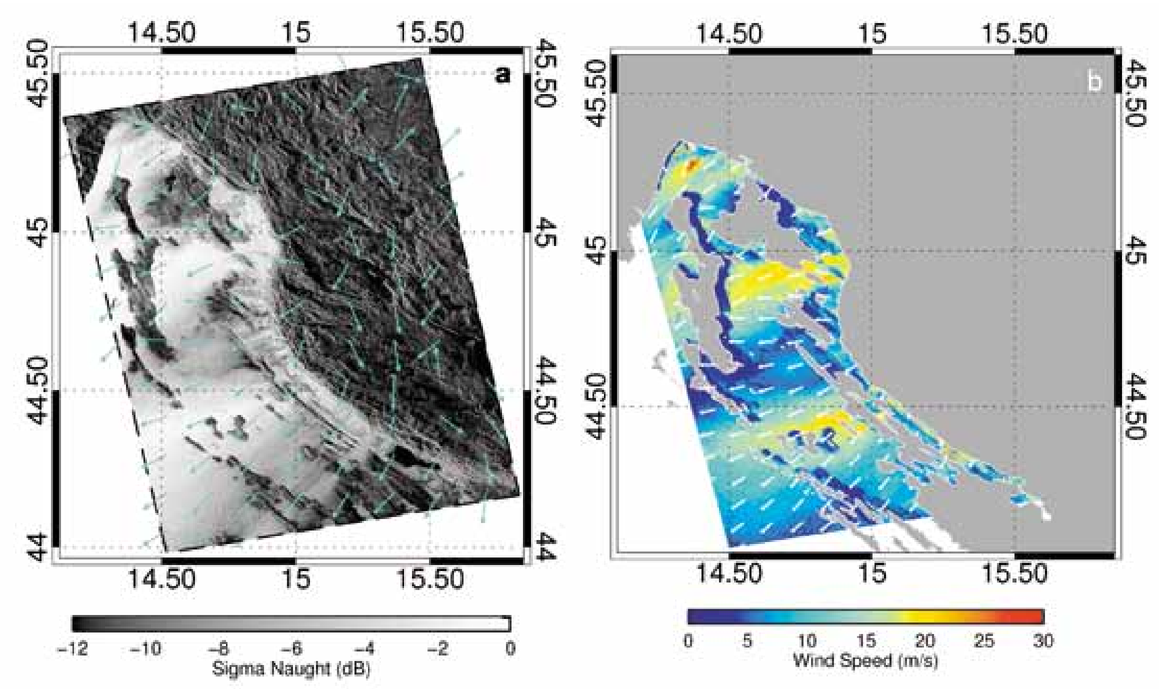


*Fig. 9. As in Fig. 6, but for 12 February 2012, 16:41 UTC. The scene incidence angle range is 19.5 – 30.3 degrees*

Scandinavia and the central Mediterranean area, including the Adriatic, experience low-pressure systems. Over the Southern Adriatic the synoptic situation is similar to that on February 4, whereas the Northern Adriatic bora is similar to the first two cases (from 2011). The response to this synoptic setup is forceful (Fig. 9), and the expected jets (Bakar/Plase, Senj/Vratnik, and Karlobag/Oštarijska) clearly distinguish themselves. Archived operational forecasts suggest that the February 4th and February 12th scenes are snapshots of a single, prolonged bora event that, while weakening and coming back, lasted until early hours of February 15th, culminating on February 11th. The SAR derived wind field is given in Fig. 9b, and the WRF model field in Fig. 4d.

## CONCLUSIONS

An early examination of the Adriatic Sea bora wind as registered in the TerraSAR-X scenes is presented in this paper. Since bora is primarily winter wind and the town of Senj is known for frequent and severe bora episodes, we focus on four TerraSAR-X scenes collected in the winter of 2011 and 2012 over the northeastern Adriatic, on the lee of Dinaric Alps stretch roughly centered on the town of Senj. Recently developed XMOD2 GMF is used for wind field derivation, whereas WRF model was employed to estimate the wind direction. The presented TerraSAR-X scenes have captured representative bora events exhibiting rich details in bora-induced jet and wake patterns in the lee of the Dinaric Alps. The preliminary results provide a strong incentive for further research and improvements on both remote sensing and the modeling side. The WRF model was used primarily to provide the needed wind direction, but the details registered even in spatially averaged normalized radar cross sections suggest the need for still higher resolution numerical simulations in order to properly capture the orographic impact on and the fine details in the surface wind field. On the other hand, comparisons of SAR derived wind with both research and operational modeling results indicate that the currently used GMF may benefit from enlarging the matchup data base with samples of severe winds. In continuation of this work we have started more formal verification of TerraSAR-X derived bora winds.

## ACKNOWLEDGEMENTS

This work has been supported by the Croatian Ministry of Science, Education, and Sport via research grants 098-0982705-2707 and 119-1193086-1311. The TerraSAR-X data have been collected within the framework of the research proposal OCE0478. We thank two anonymous reviewers whose thoughtful comments helped improve the manuscript.

## REFERENCES

ALPERS, W., A. IVANOV & J. HORSTMANN. 2009. Observations of bora events over the Adriatic Sea and Black Sea by spaceborne synthetic aperture radar. Mon. Weather Rev., 137: 1154-1165.

BELUŠIĆ, D. & Z.B. KLAIĆ. 2004. Estimation of bora wind gusts using a limited area model. Tellus A, 56(4): 296-307.

BELUŠIĆ, D. & Z.B. KLAIĆ. 2006. Mesoscale dynamics, structure and predictability of a severe Adriatic bora case. Meteorol. Z., 15: 157–168.

BELUŠIĆ, D., M. ŽAGAR & B. GRISOGONO. 2007. Numerical simulation of pulsations in the bora wind. Q. J. R. Meteorol. Soc., 133: 1371-1388. doi: 10.1002/qj.129.

BREIT, H., T. FRITZ, B. SCHATTLER, E. BORNER, M. LACHAISE, A. NIEDERMEIER, M. EINEDER & U. BALSS. 2007. TerraSAR-X payload data processing – First Experiences. Geoscience and Remote Sensing Symposium IGARSS, 23-28 July, Barcelona, Spain, 3936 pp.

CHEN, F. & J. DUDHIA. 2001. Coupling an advanced land-surface/hydrology model with the Penn State/NCAR MM5 modeling system. Part I: Model description and implementation. Mon. Weather Rev., 129: 569–585.

ENGER, L. & B. GRISOGONO. 1998. The response of bora-type flow to sea surface temperature. Q. J. R. Meteorol. Soc., 124: 1227-1244.

GOHM, A., G.J. MAYR, A. FIX & A. GIEZ. 2008. On the onset of bora and the formation of rotors and jumps near a mountain gap. Q. J. R. Meteorol. Soc., 134: 21-46.

GRISOGONO, B. & L. ENGER. 2004. Boundary-layer variations due to orographic wave-breaking in the presence of rotation. Q. J. R. Meteorol. Soc., 130: 2991-3014.

GRISOGONO, B. & D. BELUŠIĆ. 2009. A review of recent advances in understanding the meso- and micro-scale properties of the severe Bora wind. Tellus A, 61: 1-16.

GRUBIŠIĆ, V. 2004. Bora-driven potential vorticity banners over the Adriatic. Q. J. R. Meteorol. Soc., 130: 2571-2603.

HERSBACH, H., A. STOFFELEN & S. DE HAAN. 2007. An Improved C-band scatterometer ocean geophysical model function: CMOD5. J. Geophys. Res., 112; doi: 10.1029/2006JC003743.

HORSTMANN, J. & W. KOCH. 2005. Measurement of Ocean Surface Winds UsingSynthetic Aperture Radars. IEEE J. Ocean. Eng., 30: 508-515.

HORVATH, K., A. BAJIĆ & S. IVATEK-ŠAHDAN. 2011. Dynamical downscaling of wind speed in complex terrain prone to bora-type flows. J. Appl. Meteor. Climatol., 50: 1676-1691.

JIANG, Q. & J.D. DOYLE. 2005. Wave breaking induced surface wakes and jets observed during a bora event. Geophys. Res. Lett., 32, L17807, doi:10.1029/2005GL022398.

KAIN, J.S. & J.M. FRITSCH. 1993. Convective parameterization for mesoscale models: The Kain- Fritsch scheme. The representation of cumulus convection in numerical models. Meteor. Monogr., No. 24, Amer. Meteor. Soc., 165-170.

KLEMP, J.B. & D.R. DURAN. 1987. Numerical modelling of Bora winds. Meteorol. Atmos. Phys. 36: 215-227.

KUZMIĆ, M. & M. ORLIĆ. 1987. Wind-induced vertical shearing: ALPEX/MEDALPEX data and modelling exercise. Ann. Geophys., 5B: 103-112.

LEHNER, S., J. HORSTMANN & W. KOCH. 1998. Mesoscale wind measurements using recalibrated ERS SAR images. J. Geophys. Res., 103: 7847-7856.

LEHNER, S., J. SCHULZ-STELLENFLETH & S.

BRUSCH. 2008. TerraSAR-X measurements of wind fields, ocean waves and currents. ESA SP-656, Proc. of SeaSAR 2008, Frascati, Italy, 6pp.

LEHNER, S., A. PLESKACHEVSKY & M. BRUCK. 2012. High resolution satellite measurements of coastal wind field and sea state. Int. J. Remote Sens., in press.

LI, X.F., W. ZHENG, W.G. PICHEL, C.-Z. ZOU & P.C. CLEMENTE-COLON. 2007. Coastal katabatic winds imaged by SAR. Geophys. Res. Lett., 34: L03804, doi: 10.1029/ 2006GL028055.

LI, X.-M. & S. LEHNER. 2013. Algoritam for sea surface wind retrieval from TerraSAR-X and Tandem-X. IEEE Trans. Geosci. Remote Sens., DOI : 10.1109./TGRS.2013.2267780.

LIN, H., Q. XU & Q. ZHENG. 2008. An overview of SAR measurements of sea surface wind. Prog. Nat. Sci., 18: 913-919.

MONALDO, F.M. 2000. The Alaska SAR demonstration and near real-time synthetic aperture radar winds. The Johns Hopkins Apl. Tech. Dig., 21: 75–84.

MONALDO, F.M., V. KERBAOL, P. CLEMENTE-COLON, B. FUREVIK, J. HORSTMANN, J. JOHANNESSEN, X. LI,W.G. PICHEL, T. SIKORA, D.R. THOMPSON, AND C.C.WACKERMAN. 2003. The SAR measurement of ocean surface winds. In: Second Workshop on Coastal and Marine Applications of SAR, Longyearbyen, Spitsbergen, Norway

ORLIĆ, M., M. KUZMIĆ & Z. PASARIĆ. 1994. Response of the Adriatic Sea to the bora and sirocco forcing. Cont. Shelf Res., 14: 91-116.

PITZ, W. & D. MILLER. 2010. The TerraSAR-X satellite. IEEE Trans. Geosci. Remote Sens., 48: 615–622.

PULLEN, J., J.D. DOYLE, R. HODUR, A. OGSTON, J.W. BOOK, H. PERKINS & R. SIGNELL. 2003. Coupled ocean-atmosphere nested modelling of the Adriatic Sea during winter and spring 2001. J. Geophys. Res., 108(C10), 3320, doi: 10.1029/2003JC001780.

QUILFEN, Y., B. CHAPRON, T. ELFOUHAILY, K. KATSAROS & J. TOURNADRE. 1998. Observation of tropical cyclones by high-resolution scatterometry. J. Geophys. Res. 103: 7767-7786.

REN, Y., Z.S. LEHNER, S. BRUSCH, X.-M.LI & M.-X. HE. 2012. Retrieval algorithm for sea surface wind field using X-band TerraSAR-X data. Int. J. Remote Sens., 33: 7310 – 7336, doi: 10.1080/01431161.2012.685977.

SIGNELL, R.P., J. CHIGGIATO, J. HORSTMANN, J.D. DOYLE, J. PULLEN & F. ASKARI. 2010. High-resolution mapping of Bora winds in the northern Adriatic Sea using synthetic aperture radar. J. Geophys. Res., 115: C04020, doi:10.1029/2009JC005524.

SKAMAROCK, W.C., J.B. KLEMP, J. DUDHIA, D.O. GILL, D.M. BARKER, M.G. DUDA, X-Y HUANG, W. WENG & J.G. POWERS. 2008. A description of the Advanced Research WRF Version 3. NCAR Tech. Note, NCAR/TN-475+STR, 113 pp.

SMITH, R.B. 1987. Aerial observations of the Yugoslavian Bora. J. Atmos. Sci., 44: 269-297.

STOFFELEN, A. & D. ANDERSON. 1997. Scatterometer data interpretation: Estimation and validation of the transfer function CMOD4. J. Geophys. Res., 102: 5767– 5780.

VEČENAJ, Ž., D. BELUŠIĆ & B. GRISOGONO. 2010. Characteristics of the near-surface turbulence during a bora event. Ann. Geophys., 28: 155-163.

VEČENAJ, Ž., D. BELUŠIĆ, V. GRUBIŠIĆ & B. GRISOGONO. 2012. Along-coast features of bora related turbulence. Bound.-Layer Meteorol., 143:527-545. doi: 10.1007/s10546-012-9697-6

WERNINGHAUS R. & S. BUCKREUSS. 2010. The TerraSAR-X Mission and System Design. IEEE Trans. Geosci. Remote Sens., 48: 606–614.

Received: 19 July 2012
Accepted: 27 March 2013

# Opažanja sjeveroistočno-jadranske bure pomoću satelita TerraSAR-X: rani rezultati

Milivoj KUZMIĆ[1*], Xiao-Ming LI[2], Branko GRISOGONO[3], Igor TOMAŽIĆ[1] i Susanne LEHNER[2]

[1]*Institut Ruđer Bošković, Zavod za istraživanje mora i okoliša, Laboratorij satelitske oceanografije, Bijenička cesta 54, 10002 Zagreb, Hrvatska*

[2]*Njemački aero-svemirski centar (DLR), Centar za promatranje Zemlje (EOC), Institut za tehnologije daljinske detekcije (IMF), Oberpfaffenhofen D-82234 Wessling Njemačka*

[3]*Sveučilište u Zagrebu, Prirodoslovno-matematički fakultet, Geofizički odsjek Andrija Mohorovičić, Horvatovac bb, 10000 Zagreb, Hrvatska*

[*]*Kontakt adresa, e-mail: kuzmic@rudjer.irb.hr*

## SAŽETAK

U radu su prikazani rani rezultati detekcije bure na sjeveroistočnoj strani Jadrana pomoću satelita TerraSAR-X. TerraSAR-X je njemački satelit lansiran 2007. godine koji nosi „phased- array" radar sintetičke aperture (SAR) s mogućnošću rada uz različite polarizacije i uz više načina snimanja. Povratno zračenje instrumenta SAR može se iskoristiti za određivanje polja vjetra uz prostorno razlučivanje koje ne omogućuje ni jedan drugi instrument. Područja niskih mlaznih struja i zavjetrinske tišine, uzrokovana terenom, posebno su podatni za ispitivanja pomoću instrumenta SAR. Bura - hladan, suh i jak planinski vjetar koji puše iz sjeverno istočnih smjerova na istočnoj strani Jadranskog mora, izaziva spomenuti odziv. Kako je bura primarno zimski vjetar a senjsko područje poznato po čestim epizodama olujne bure, rad je fokusiran na TerraSAR-X scene registrirane tijekom zima 2011. i 2012. godine u širem području približno centriranom na Senj. Nedavno razvijena geofizička modelska funkcija XMOD2 korištena je za određivanje brzine vjetra a WRF model za procjenu njegova smjera. Odabrane TerraSAR scene pokrivaju reprezentativne epizode bure te pokazuju bogatstvo detalja u daljinskim zapisima niskih mlaznih struja i zavjetrinskih struktura koji nastaju na jadranskoj strani Dinarida. Detalji zabilježeni u odzivnom normaliziranom radarskom presjeku uvjerljivo sugeriraju potrebu još boljeg prostornog razlučivanja u numeričkim simulacijama da bi se ispravno modeliralo orografski utjecaj i detalje pripovršinskog polja vjetra. Usporedbe s rezultatima, kako istraživačkog tako i operativnog modeliranja, ukazuju da bi proširenje baždarne baze podataka uzorcima olujnog i orkanskog vjetra moglo poboljšati geofizičku modelsku funkciju.

**Ključne riječi:** TerraSAR-X, Jadran, bura